

Dynamical state of the network determines the efficacy of single neuron properties in shaping the network activity

Ajith Sahasranamam^{1,2}, Ioannis Vlachos^{1,2}, Ad Aertsen², and Arvind Kumar^{1,2,*}

⁵ Bernstein Center Freiburg and Faculty of Biology, University of Freiburg, 79104 Freiburg, Germany.

⁶ Computational Biology, School of Computer Science and Communication, KTH Royal Institute of Technology,
⁷ Stockholm, 10044, Sweden

⁸ *arvkumar@kth.se

ABSTRACT

Spike patterns are among the most common electrophysiological descriptors of neuron types. Surprisingly, it is not clear how the diversity in firing patterns of the neurons in a network affects its activity dynamics. Here, we introduce the state-dependent stochastic bursting neuron model allowing for a change in its firing patterns independent of changes in its input-output firing rate relationship. Using this model, we show that the effect of single neuron spiking on the network dynamics is contingent on the network activity state. While spike bursting can both generate and disrupt oscillations, these patterns are ineffective in large regions of the network state space in changing the network activity qualitatively. Finally, we show that when single-neuron properties are made dependent on the population activity, a hysteresis like dynamics emerges. This novel phenomenon has important implications for determining the network response to time-varying inputs and for the network sensitivity at different operating points.

11 Introduction

12 Neurons express a large diversity in terms of their biochemical, morphological and electrophysiological properties.^{1–4}
13 However, it is not clear if and under which conditions such diversity plays a functional role. It has been shown that
14 selective stimulation of neurons of a given type expressing specific bio-markers can modulate different aspects of brain
15 function.⁵ For instance, selective stimulation of neurons changes the excitation/inhibition balance,⁶ network dynam-
16 ics^{7,8} and computations performed by the network,⁹ thereby leading to an altered animal behaviour. Moreover, noise
17 introduced by intrinsic properties of neurons/synapses can have several effects. It can render the dynamics more robust
18 to perturbations¹⁰ and can improve the encoding and decoding of neuronal activity by reducing correlations.¹¹ These
19 experiments provide strong support to the ‘neuron doctrine’ and motivate the search for novel bio-markers and specific
20 functions of different classes of neurons.^{4,12} However, experiments also suggest that stimulation of a certain neuron type
21 may not cause any discernible change in the population activity and animal behaviour.¹³ Moreover, detailed models of
22 single neurons¹⁴ and networks¹⁵ have shown that multiple combinations of neuron and synapse parameters can lead to
23 similar activity states;¹⁶ suggesting that exact neuronal properties are not crucial to obtain a specific dynamical network
24 state and, hence, a specific function.

25 These conflicting studies make it important to identify: (1) Changes in which of the neuron properties can affect the
26 network dynamics? (2) In which dynamical states is the network activity susceptible to changes in a certain neuronal
27 property? Here we focus on the effect of spike bursting on the network activity dynamics and vice versa. Spike bursting
28 is a common electrophysiological descriptor of a neuron type^{17,18} and the fraction of bursting neurons depends on the
29 brain region¹⁹ and even in a given brain region the firing rate of spike bursts may change depending on their inputs²⁰
30 and on the behavioral task.²¹ Finally, the rate and fraction of burst spiking increases in epilepsy²² and Parkinson’s
31 disease.²³ From a dynamics perspective, when neurons operate in an ‘integration mode’, temporal integration of spike
32 bursts can qualitatively change the response of post-synaptic neurons and, consequently, of the network. Such effects
33 could be further amplified by short-term dynamics²⁴ and long-term plasticity of the synapses.^{25,26} Therefore, the burst
34 firing pattern, which is very different from the spike trains of the leaky-integrate-and-fire (LIF) neuron model is a suitable
35 candidate to study the influence of single neuron firing patterns on the network activity. Surprisingly, despite this wealth
36 of literature on the effects of neuronal and synaptic properties on network dynamics (see review by Wang²⁷), it is not
37 at all clear how firing patterns of various neuron types may affect the network dynamics and how network dynamics, in
38 turn, may help shape neuronal firing patterns.

39 Here, we present an analytical framework to study the effect of spike bursting on the network dynamics. Using
40 mathematical analysis and numerical simulations of large-scale network models of spiking neurons we investigate the
41 effects of firing patterns – exemplified here by bursting activity of inhibitory neurons – on network synchrony and oscillations.
42 Our analysis shows that there are two different mechanisms by which spike bursting can affect the network dynamics.
43 We show that single-neuron burst firing is most effective in changing the network state when the latter is in a transition

44 zone between asynchronous and synchronous firing regimes. That is, the effect of single-neuron bursting is contingent
45 on the network activity state itself. Thus, our results suggest that the brain can exploit the heterogeneity of neuronal
46 spike patterns if it operates in the transition zones between different activity regimes.

47 Finally, we show a novel property of hysteresis in the network activity, caused by the mutual interactions between
48 single-neuron firing patterns and network dynamics. Hysteresis implies that the network output does not only depend on
49 the current input but also on previous network states and that under certain conditions the network output will change
50 slowly compared to the input. This will influence the network sensitivity at different operating points and, thereby, the
51 network response to time-varying inputs.

52 Results

53 Previous models have addressed the issue of neuronal and synaptic diversity by drawing values from various parameter
54 distributions instead of assigning single values. The specific effect of neuronal heterogeneities in random networks becomes
55 more apparent when instead of a distribution of neuron parameters, different types of neurons are used.²⁸ Therefore, to
56 study the effect of spike patterns of individual neurons, we characterised the activity of a randomly connected network of
57 excitatory (*E*) and inhibitory (*I*) neurons by systematically increasing the fraction of one type of neuron in the inhibitory
58 population. This manipulation was motivated by two experimental observations: (1) the fraction of bursting neurons
59 depends on the brain region,¹⁹ (2) the probability of a neuron to elicit spike bursts depends on the inputs²⁰ and neurons
60 can dynamically switch their firing mode, depending on the context^{21,29} and, more permanently, in the case of specific
61 brain diseases.^{22,23} That is, the fraction of bursting neurons is a dynamical variable which may change, depending on
62 the behavioral context, inputs, brain region and brain condition. We considered a sparse Erdos-Renyi (ER) type network
63 of *E* and *I* neurons connected with 10% probability. This choice of ER type random networks ensured that our results
64 are not dependent on any specific connectivity of the bursting neurons. We used the Izhikevich neuron model for its
65 computational efficiency and its ability to reproduce nearly all spike patterns observed *in vitro*.³⁰ All excitatory neurons
66 were realised as regular spiking neurons. The inhibitory neuron population consisted of *F*% burst spiking neurons (BS)
67 and (100 – *F*)% fast spiking (FS) neurons.

68 Effect of bursting on the stability of oscillatory activity

69 We first characterised the effect of bursting neurons on γ band oscillations in recurrent networks. These oscillations are
70 considered to play a crucial role in brain function.^{31–33} We tuned the parameters - external input rate and synaptic
71 weights - of a network of RS excitatory and FS inhibitory neurons (i.e. *F* = 0) to obtain stable γ band oscillations^{34,35}
72 (Fig. 1B). In this regime, individual neurons do not produce an action potential in every oscillation cycle and, thus, have
73 a mean discharge rate that is typically lower than the frequency of the fast gamma rhythm emerging at the network
74 level.³⁶ These oscillations are known to be robust to heterogeneities (when modeled by a unimodal distribution of neuron
75 parameters) and noise in the external input.^{36–38} In the following, we study the stability of these oscillations in a network

76 with two or three different types of neurons.

77 When all inhibitory FS neurons were replaced by BS neurons, with all other parameters kept constant as in (Fig.1B),
78 the oscillations were severely weakened (Fig.1C). For an intermediate fraction of BS neurons ($F = 0.2$), the oscillations
79 were not completely diminished, but the stability of the oscillations was severely affected and short oscillatory epochs were
80 interrupted by non-oscillatory activity. To quantify the stability of the oscillations, we estimated the spectral entropy (H_s)
81 of the population activity spectrum, which provides a measure of the dispersion of the spectral energy of a signal (see
82 Methods). We found that the spectral entropy increased with the fraction of BS neurons and saturated to its maximum
83 value (Fig. 1D). Irrespective of the strength of the external input (η), about 30% BS neurons were sufficient to quench
84 the oscillations (Fig. 1D).

85 For a fixed proportion of BS and FS neurons, the excitatory input strength η shifted the operating point of the
86 network by increasing the firing rate of the individual neurons (Fig. 1E). This also resulted in an increase in the dominant
87 oscillation frequency (60 – 100 Hz), however, the spectral entropy remained unaffected (Fig. 1F). Thus, it is likely that
88 the reduction in oscillation power is a consequence of the spike pattern of the BS and not of the different $f - I$ curve of
89 the BS neurons. Unfortunately, though, it is not trivial to separate the contribution of the spike patterns and the $f - I$
90 curve to the network activity state. As we will show later, the effect of spike patterns and $f - I$ curve can be separated
91 by adapting the standard LIF neurons.

92 Response of network activity to single neuron bursting

93 In the above, we showed the effect of BS neurons on the oscillatory dynamics of a random network only for a specific
94 activity regime of the network. Sparsely connected random networks of excitatory and inhibitory neurons can exhibit
95 distinct activity states depending on the external excitatory input (η) and the ratio of recurrent inhibition and excitation
96 (g). While individual neurons can fire in a regular (R) or irregular (I) manner, the population activity can be synchronous
97 (S) or asynchronous (A). Thus, the network activity could be either AI, SI, AR, or SR.^{39,40} In the mean-driven regime
98 the neurons fire in a regular manner whereas in the fluctuation driven regime their spiking becomes irregular. Because
99 neuronal activity *in vivo* is irregular, only SI and AI are biologically relevant for information processing. Therefore, we
100 studied how the AI and SI activity regions in the parameters space of η and g are changed when FS are systematically
101 replaced by BS neurons (Fig. 2A-C). The parameters η and g were varied to obtain low to mid-range firing rates (
102 ≤ 25 spikes/sec) and irregular spiking in the RS neurons ($CV_{ISI} \geq 0.5$).

103 Replacement of FS neurons by BS neurons altered the various regions in the network parameter space differently. We
104 identified four different ranges of parameters giving rise to four distinct modulations of activity regimes (see Fig. 2D,E):
105 (1) A parameter range in which the network remained in the synchronous state, irrespective of the fraction of BS neurons.
106 This invariance of the synchronous network activity to the neuron types was observed for small values of g . In a network
107 where all neurons have identical $f - I$ curve, this parameter regime would correspond to a mean-driven regime. This
108 classification is, however, not directly applicable here, because FS and RS neurons have different slopes of their $f - I$

109 curves. (2) A parameter range in which the network remains in an asynchronous state, irrespective of the fraction of
110 BS neurons. In this regime, g is large enough to drive the network into the fluctuation-drive state, resulting in irregular
111 and asynchronous (non-oscillatory – $H_S \geq 0.6$) firing. (3) The network activity makes a transition from the synchronous
112 to the asynchronous state, that is, BS neurons tend to weaken or even quench the weak synchrony. (4) In a relatively
113 small parameter regime, we also observed that for a small fraction of BS neurons, the network activity changed from
114 the synchronous to the asynchronous state (similar to (3)), but for a larger fraction of BS neurons, the activity returned
115 to the synchronous state again. That is, for 100% BS or FS neurons, the network remained in a synchronous (also
116 oscillatory, $H_S \leq 0.6$) state, whereas for intermediate fractions the network synchrony was destroyed ($H_S \geq 0.6$).

117 The Izhikevich neuron in its bursting mode, differs from its fast-spiking mode in two respects: it produces more
118 than one spike every time the membrane potential crosses the spiking threshold (see Fig. 3A) and the $f - I$ curve of the
119 bursting neurons has a larger slope than that of the FS neurons (see Fig. 3B). In the existing neuron models (Izhikevich
120 neuron model, generalised integrate-and-fire neuron), it is not possible to change the $f - I$ curve of the neuron without
121 affecting its firing pattern.

122 **The state-dependent stochastic bursting neuron model**

123 To understand the role of spike patterns in shaping the network dynamics it is important to isolate their effects from
124 the different $f - I$ curves. Therefore, we modified the standard LIF neuron model to produce bursting of B spikes in a
125 stochastic manner with a probability $1/B$ every time its membrane potential reaches the spiking threshold (see Methods).
126 We refer to this new model as the State-dependent Stochastic Bursting Neuron (SSBN) model when the parameter B
127 depended on the input level. In a special case, B could be a fixed number. The SSBN model not only ensures that the
128 $f - I$ curves of the bursting and fast-spiking neurons remain identical (Fig. 3D), but it also allows us to change the size and
129 the duration of the burst without cumbersome parameter tuning (Fig. 3C). Moreover, unlike the Izhikevich neuron model
130 and the generalised LIF model, which are often used to model bursting dynamics of neurons, the bursting characteristics
131 of the SSBN remain unchanged, irrespective of the input statistics. The response characteristics of the SSBN are similar
132 to that of the LIF, except that an increase in the number of spikes per burst B decreases the high-frequency firing limit
133 of the neuron (Supplementary Fig. S1).

134 **Effects of different firing patterns of inhibitory neurons on the stability of network oscillations**

135 In contrast to FS neurons, BS neurons spike in bursts, but for the same input the total number of spikes generated by
136 a BS neuron is identical to that of an FS neuron. This implies that in the SSB neuron, spikes are clumped together,
137 creating 'empty' temporal windows (with a duration depending on burst size) in which no spikes occur (Fig. 3C) and very
138 short windows in which the number of spikes produced will be significantly higher than that of FS neurons. Therefore,
139 while an FS neuron exerts a relatively uniform inhibition onto its post-synaptic neurons, BS neurons exert inhibition in
140 clumps. Because of the temporal clustering of spikes in BS neurons, two distinct mechanisms emerge that define the

141 stability of the oscillatory and asynchronous states, respectively.

142 **Stability of the oscillatory state: Additional spikes part of the burst disrupt oscillations**

143 Fast (or γ) oscillations could be described as 'interneuron generated' (ING) or pyramidal-interneuron generated (PING).³⁷
144 In the ING oscillations, recurrent inhibition of the inhibitory interneurons creates a small time window for pyramidal
145 neurons to spike. In the PING mechanism, an increased activity of pyramidal neurons causes an increase in the activity of
146 inhibitory interneurons, which subsequently inhibit the pyramidal neurons. In both mechanisms, inhibition sets the time
147 window for the activation (ING) or inactivation (PING) of the pyramidal neurons.⁴¹ The temporal clustering of spikes in
148 BS neurons causes a temporal jitter in the duration of the recurrent inhibition and, therefore, weakens the oscillations
149 (mechanism-I).

150 This is best illustrated in the case of ING oscillations. Here, the initiation of a burst at the edge of the preceding
151 oscillation cycle distorts the subsequent window of opportunity for the next inhibitory cycle and, consequently, the
152 oscillation is quenched in the inhibitory population. This renders the excitatory population non-oscillatory as well.

153 To demonstrate this mechanism, we simulated a simple E-I network with an inhibitory population composed of FS
154 neurons only. The values of g and η were adjusted to render the network in the ING oscillation regime. Based on
155 thresholding the Z-scored PSTH of the population activity, the oscillatory cycles were marked (gray stripes in Fig. 4A).
156 Next, we simulated the network once more with identical parameters, except that at the fifth oscillatory cycle (Fig. 4
157 A), 40% of FS neurons were replaced by BS neurons. By comparing these two simulations, we determined the number
158 of 'additional' inhibitory spikes (num_{add}) that fell outside the oscillatory window.

159 To mimic the effect caused by the additional spikes generated by the BS neurons, we added num_{add} additional
160 inhibitory spikes at the exact moment when a particular inhibitory oscillatory cycle tapered off (Fig. 4B). This time was
161 determined by running an identical simulation with the same random number generator seeds (baseline) (Fig. 4C pale
162 blue trace). Addition of the previously determined number of extra inhibitory spikes (as would happen in a BS neuron)
163 indeed disturbed the next oscillatory cycle significantly (Fig. 4C blue trace).

164 To test whether it is the timing of the bursts that weakens the oscillations and not the number of spikes contained
165 in them, we added the same number of additional inhibitory spikes during the peak of the preceding inhibitory oscillatory
166 cycle (control). In this case, the oscillation amplitude and frequency were not significantly changed (Fig. 4C dark blue
167 trace), thereby showing that only the timing of the bursts (or the corresponding additional spikes) destroyed oscillations.
168 A similar distortion of oscillations is observed when adding additional spikes in the inhibitory population in a network
169 in which oscillations are driven by the PING mechanism (Fig. 4E) (scheme in Fig. 4D). The breakdown of oscillations
170 by temporal jitter of inhibition is effective when oscillations are weak. In strongly oscillatory states, the effective synaptic
171 couplings are strong and, hence, jittering of inhibition is not sufficient for quenching oscillations (see also Supplementary
172 Fig. S2B).

173 **Stability of the asynchronous state: Bursting makes the network susceptible to oscillations**

174 When spikes arrive in a burst, the post-synaptic neuron receives a much bigger compound PSP due to the temporal
175 summation of individual spikes. Because we preserved the $f - I$ curve of the neuron while making it bursting, effectively
176 each spike was replaced by B spikes while reducing the input rate by a factor B . This is equivalent to a network of
177 non-bursting neurons connected with a synaptic kernel that reflects the temporal summation of spikes in the burst. This
178 analogy allows us to use the established mean-field theory to investigate the stability of the AI state of the network
179 activity.^{36,38} Only when the compound PSP renders the AI state to become unstable, we would expect bursting neurons
180 to transform the AI state into the SI state, otherwise a change in the neuron spiking behavior will not affect the network
181 activity.

For simplicity in our network we kept the recurrent synaptic coupling strengths as $J_{EE} = J_{IE} = J_E$ and $J_{II} = J_{EI} = J_I$,
and $J_I = g \cdot J_E$ (where the subscript xy indicates a connection from the y population to the x population). To check
for the stability of the AI state, we introduced a small perturbation in the steady-state firing rate r_{P_0} of population P
(excitatory or inhibitory),

$$r_P(t) = r_{P_0} + Re[\hat{r}_{P_1}(\lambda)e^{\lambda t}]$$

where $\lambda = x + j\omega$ with ω being the modulation frequency. The perturbation in the steady-state firing rate leads to a
perturbation in the recurrent synaptic input

$$I_P(t) = I_{P_0} + Re[\hat{I}_{P_1}(\lambda)e^{\lambda t}]$$

182 where I_{P_0} is the baseline steady state synaptic input, $\hat{I}_{P_1}(\lambda) = J_IS_I(\lambda)\hat{r}_{I_1} + J_ES_E(\lambda)\hat{r}_{E_1}$, and S_I and S_E are the synaptic
183 response functions.³⁸

184 Subsequently, the perturbation in the synaptic input would change the network firing rate by $R_P(\lambda)\hat{I}_{P_1}(\lambda)$ (where
185 $R_P(\lambda)$ is the neuron response function³⁸). In a recurrent network, if the rate perturbation, \hat{r}_{P_1} is equal to the synaptic
186 input perturbation, the perturbation does not die out, indicating an instability of the asynchronous state. That is, for an
187 unstable asynchronous state:

$$\hat{r}_{P_1}(\lambda) = R_P(\lambda)\hat{I}_{P_1}(\lambda)$$

188 We used the above equation to derive the conditions for the instability of the AI state by analyzing the following

189 equation:³⁸

$$J_E \cdot [R_E(\lambda) \cdot S_E(\lambda) - R_I(\lambda) \cdot S_I(\lambda) \cdot g] = 1 \quad (1)$$

190 where $g = \frac{J_I}{J_E}$. If the synaptic coupling strength J_E crosses a critical J_{cr} , the asynchronous activity destabilizes and
191 the network activity enters an oscillatory regime. Because of the temporal summation of burst spikes, when BS neurons
192 replace FS neurons in the inhibitory population, the inhibitory synaptic response function S_I is altered. Specifically, an
193 increase in the number of spikes per burst leads to an increase in the effective synaptic rise time (see Methods). This in
194 turn, leads to a reduction of the critical coupling value J_{cr} , rendering the AI state unstable (see Fig. 5 A – black dotted
195 line). Thus, if $J_E < J_{cr}$ for $B = 1$ and $J_E > J_{cr}$ for $B = 4$, a change of neuron type from FS ($B = 1$) to BS ($B = 4$) will
196 destabilize the AI state and lead the network activity into an oscillatory state. However, if J_E remains below J_{cr} for $B = 1$
197 and $B = 4$, the network remains in the asynchronous state, despite the replacement of FS by BS neurons. If the network
198 with FS neurons is already in a synchronous state ($J_E > J_{cr}$), a replacement of all of the FS neurons with BS neurons
199 will not affect the state. However, if the oscillations are weak, replacement of a certain fraction of FS neurons with BS
200 neurons can destroy oscillations through mechanism-I by temporal jitter of inhibition. Thus, in the asynchronous activity
201 state BS neurons affect the network dynamics by reducing the value of the critical coupling (J_{cr}), leading to a shift from
202 asynchronous to synchronous network activity (mechanism-II). As equation-1 indicates, whether or not BS neurons will
203 change the asynchronous activity state to the oscillatory state by mechanism-II depends on the network connectivity
204 parameters and the firing rate of the network r_0 .

205 Effect of spike bursting on the network activity dynamics

206 The understanding of how BS neurons or spike bursts affect the network dynamics allowed us to re-examine the change
207 in the dynamics of a recurrent network when FS neurons are systematically replaced by BS neurons. We simulated a
208 random recurrent network with SSB neurons and studied the robustness of the synchronous and asynchronous states
209 when single spiking SSB neurons (equivalent to FS neurons) were systematically replaced by SSB neurons with spike
210 bursts of size four (equivalent to BS neurons).

211 When the network was tuned to be in an oscillatory regime ($J_E > J_{cr}$), an increase of the number of bursting neurons
212 first lead to a non-oscillatory network activity ($H_S \approx 0.75$, $F = 25\%$). This weakening of the oscillations is a result
213 of mechanism-I. However, as the fraction of BS neurons was further increased ($F \geq 50\%$), mechanism-II became more
214 effective and counteracted mechanism-I, resulting in oscillatory network activity again ($H_S \approx 0.5$) (see Fig. 5B). This
215 non-monotonic change in H_S resembles the non-monotonic change in networks with the Izhikevich model neuron (see
216 Fig. 1A-C). Based on our observations made in networks with SSB neurons, we think that even in a network with Izhikevich
217 model neurons, the non-monotonic state changes were largely governed by the change in neuron spike patterns. Note

218 that a network can remain in the synchronous state for all values of F , provided that the inputs to the excitatory and
219 inhibitory populations are appropriately controlled (see Supplementary Fig. S2B).

220 When the network was tuned to be in an asynchronous non-oscillatory state with weak correlations ($H_S \approx 0.7, J_E < J_{cr}$),
221 replacing FS neurons by BS neurons rendered the network in an oscillatory state. The spectral entropy monotonically
222 decreased with the fraction of BS neurons (see Fig. 5B). Hence, the transformation of non-oscillatory activity to the
223 oscillatory state was governed purely by mechanism-II.

224 In a network with highly aperiodic activity and very weak correlations ($H_S \geq 0.8, J_E \ll J_{cr}$), i.e. when the activity is
225 deep in the AI regime, the network state was robust to changes in the spike pattern properties of individual neurons(see
226 Fig. 5A).

227 These results clearly show that neuron spike patterns can indeed change the network state, from a weakly non-
228 oscillatory asynchronous state to synchronous oscillations (by mechanism-II) and vice versa (by mechanism-I). At the
229 same time, a non-oscillatory state with very weak correlations is invariant to changes in the neuron spike pattern properties.
230 We conclude that network activity is susceptible to neuron spiking patterns only in the transition zone between different
231 regimes (here between asynchronous–non-oscillatory and synchronous–oscillatory) and the effect of neuron spike pattern
232 properties on the network activity dynamics is contingent on the network activity state itself.

233 **Bursting activity increases the population firing rate**

234 The bursting firing pattern of the inhibitory neurons aids in the transition of the network activity from the asynchronous
235 to the synchronous state (Fig. 5A). This change in the stability of the network activity also influences the population
236 firing rate (Fig. 6). The increasing 'burstiness' of the constituent bursting neurons steers the network activity into an
237 oscillatory state. This switch is accompanied by an increase in the population firing rate.

238 Additionally, the difference in the temporal structure of bursting could also change the statistics of the total synaptic
239 inputs and the output firing rate of a postsynaptic neuron. To test this, we fixed the number of bursts of an SSB neuron
240 and connected it to a LIF neuron that also received excitatory Poisson input. We measured the output firing rate and
241 variance of the free membrane potential v_{fr} of the post-synaptic LIF neuron as a function of the number of spikes in
242 a burst (Supplementary Fig.S3). The mean v_{fr} remained constant as the number of spikes in a burst was increased,
243 because irrespective of burst size the total numbers of excitatory and inhibitory spikes were preserved. However, the
244 temporal clustering of BS spiking increased the variance of v_{fr} , resulting also in an increase of the output firing. At the
245 network level, this could also contribute to an increase in the population firing rate, thereby reducing J_{cr} and, hence,
246 contributing to the switch of activity from the asynchronous irregular to the oscillatory state by facilitating mechanism-II.

247 **State dependent bursting of inhibitory neurons induces hysteresis in the network dynamics**

248 In the above, we made the assumption that the number of spikes in a burst of the SSB neuron is fixed. In real neurons,
249 where spike bursting is governed by the voltage-dependent ion channels and interactions between soma and distant tufts

250 (e.g. in pyramidal neurons²⁰), the number of spikes in a burst would depend on the network activity level. Consistent
251 with this, recent experiments indeed show that bursting can change, depending on the behavioural task and the network
252 activity state²¹ in both excitatory and inhibitory cells. In simulations with networks of Izhikevich neurons, we found the
253 'burstiness' of BS neurons also to be dependent on the network activity state (Supplementary Fig. S4).

254 To implement such state-dependence of burst size, we quantized the firing rate of the excitatory neurons into five
255 disjunct ranges ($I_B = (B-1) \times 5 - B \times 5$ spikes/sec., with $B \in \{1,2,3,4,5\}$). The SSB neuron generated B spikes per burst,
256 depending on the level of the firing rate of the excitatory neurons.

257 With this model of state-depending bursting in inhibitory neurons, we further explored the relationship between the
258 network level and neuron level properties. Usually, stationary Poisson inputs are used to determine the steady state of
259 the network activity. However, such steady state will not reveal any effects introduced by state-dependent bursting of
260 inhibitory neurons. Here we introduced dynamical changes in the network activity by slowly varying the external input
261 (100 spikes/sec per observation window 3 sec or 200 ms; see Methods).

262 Random recurrent network without any state-dependent changes in neuron properties rapidly follow changes in the
263 external input⁴² (Fig. 6A, black dots). By contrast, networks with SSBNs, exhibited hysteresis, that is, when the input
264 was changed slowly, the response of the network depended not only on the current input value but also on its history
265 (Fig. 6A,B orange dots).

266 To understand the hysteresis observed here, it is important to recall that the change in the population firing rate in
267 the system was determined by two factors: (1) a change in the external input, and (2) a change in the number of spikes
268 per burst (B) of the SSB neurons. An increase in the external input rate led to an increase in the network population
269 firing rate, until SSB neurons started to burst. Therefore, any further change in the network firing rate was governed
270 by both the further rising input rate and the increasing effect of neuron bursting. Moreover, every time B was increased
271 (see Methods), the network activity rapidly jumped (Fig. 6 A). At the peak network output firing rate, when the SSB
272 neuron elicited 5 spikes per burst, the increase in the network firing rate was dominated by the increase in B . In this
273 network state, a reduction of the external input had only a very weak effect in decreasing the population firing rate, until
274 the network firing rate had dropped enough to reduce the burst size. Once the activity dropped below this range, it
275 rapidly returned to the baseline state. In the case of a network with a small fraction of BS neurons (20%), the increase in
276 network firing rate due to the change in B was very small (Fig. 6A black dots), resulting in very little difference between
277 the network responses during the increasing and decreasing cycles of the external input.

278 Balanced random networks, which are often used to model cortical network activity, do not exhibit such hysteresis
279 properties in biologically relevant activity regimes such as the asynchronous-irregular or synchronous-irregular states.^{39,42}
280 However, under some special conditions, such as clustered connectivity⁴³ and plastic synapses,^{44,45} spiking neuronal
281 networks can exhibit bistability that may lead to hysteresis as well. Hysteresis in network activity implies slow dynamics.
282 On the one hand, bursting increases the sensitivity of the network to slowly varying changes, but on the other hand,

283 hysteresis could result in a persistent activity – that is, a change in network response activity, lasting long after the
284 stimulus originally inducing it has passed.

285 Discussion

286 A specific neuron type has a functional significance only if it has a discernible effect on the network activity state. At
287 the level of spiking activity, the effect of neuronal parameters can be described in terms of changes in the firing pattern
288 (e.g. bursting and non-bursting) and $f - I$ curve (Fig. 7A). Here, we investigated when and how neuronal spike bursting,
289 one of the most common descriptors of neuronal types, can introduce a qualitative change in network activity. Our
290 theoretical analysis and numerical simulations of neuronal networks show that the impact of spike bursting is contingent
291 on the network activity state (schematically shown in Fig. 7B). The change in the network activity state caused by the
292 temporal clustering of spikes in BS neurons can be understood in terms of two mechanisms (Fig. 7A,B). When the network
293 operates in a moderately oscillatory regime (spectral entropy ≈ 0.5), spike bursts distort the temporal relation between
294 the excitation and inhibition necessary for these oscillations^{37, 41} and, therefore, weaken the oscillations (mechanism-I).
295 In this regime, BS neurons increase the noise, thereby weakening oscillations (Fig. 4, Fig. 7B). On the other hand, spike
296 bursting reduces the effective coupling strength J_{cr} (see eq. 1), causing the asynchronous activity state to destabilize
297 (mechanism-II). That is, bursting reduces the region in the network parameter space for which asynchronous activity is
298 stable (Fig. 5, Fig. 7B). These two mechanisms are most in effect when the network activity is in a region in the activity
299 state space, close to the border between asynchronous and oscillatory states. By contrast, the highly asynchronous and
300 fully synchronous states remain unaffected by the change in the neuron spiking behavior caused by 'replacing' FS neurons
301 by BS neurons.

302 Functional consequences of a bursting dependent network state change

303 We showed that weak oscillatory activity is especially susceptible to spike bursting and that even a low fraction of BS
304 neurons ($\approx 30\%$) in the inhibitory population is sufficient to quench oscillations (mechanism-I). Such a transient increase
305 in the activity of BS neurons could form a powerful mechanism to reset network oscillations. Network oscillations in
306 the γ band (30-80 Hz) are considered to form the basis of selective communication between weakly connected brain
307 regions.^{32, 41} Bursting-induced phase resetting could be a powerful mechanism to stop or start a communication between
308 two such brain regions. Recent experiments show that bursting does indeed increase in a task-dependent manner and
309 that it synchronizes activity between different brain areas.²¹ Our results provide two potential mechanisms that can
310 act to induce phase-resetting and/or phase-synchronization and, therefore, provide a first theoretical account for these
311 experimental findings.

312 In our study, we did not incorporate any specific connectivity of the bursting neurons and, therefore, may have
313 underestimated the effect of spike bursting on the network dynamics. Recent experimental data suggest that neurons
314 exhibiting different firing patterns may receive inputs from different sources.⁴⁶ Given that neuronal connectivity is a

315 key determinant of the effect a given a neuron has on the overall network dynamics,^{47–50} the effects of spike bursting
316 on network activity would be further accentuated when bursting neurons make more specific connections, which might
317 possibly form in networks with activity dependent synaptic plasticity (Fig. 7A).

318 Network hysteresis

319 Spike bursting could be an intrinsic property of neurons⁵¹ or emerge as a consequence of network activity.^{20,21} In our
320 simulations, when we made the burst size dependent on the average firing rate in the network, we observed a hysteresis-
321 like behaviour for time-varying inputs (Fig. 6). Classical balanced random networks closely track the dynamics of the
322 external input and do not show such behaviour - in fact, a hallmark of their behaviour is to track an arbitrarily fast
323 external input.⁴² Interestingly, the speeding up or slowing down of network dynamics due to the presence of bursting
324 neurons has also been observed in other complex networks with bursting communication patterns for specific network
325 configurations.⁵²

326 To the best of our knowledge this is the first demonstration of hysteresis in Erdos-Renyi random recurrent network
327 models of cortical networks, with weak static synapses and sparse connectivity.^{27,39} Typically, in network models, low-
328 level neuron and synapse properties affect network dynamics and not the reverse, as we have shown here. Notable
329 exceptions are networks with plastic synapses⁵³ and conductance-based synapses.⁴⁰ Hence, we suggest that searching
330 for hysteresis-like behaviour in experiments could be a promising approach to identify mutually causal influences between
331 low-level neuron properties and high-level network dynamics.

332 When the size of the spike burst and the network activity are mutually dependent, the network gain depends both on
333 the network activity state and the history of the input. This is quite unlike the conventional balanced random networks,
334 where the input history plays no role in determining the network gain. More work is needed to fully understand how such
335 input-history-dependent changes in the network gain will affect the processing of time-varying input signals.

336 Finally, we speculate that disease-related aberrant neuronal activity could be a consequence of an increased fraction of
337 bursting neurons, e.g. in Parkinson's disease²³ and epilepsy.²² In these cases, possible treatments could aim at identifying
338 and counteracting the precise mechanisms of bursting activity, either pharmacologically or through electrical stimulation.

339 Conclusions

340 In summary, bursting neurons may play a crucial role in coordinating communication between different brain areas, by
341 affecting the oscillation phase of network oscillations, they may induce hysteresis and, thereby, persistent activity in the
342 networks, and they could even alter the global activity state of the network. From this, it is evident that single neuron
343 properties have a significant impact on network dynamics, but this is possibly only the case in certain network activity
344 regimes. Therefore, the effects of low level neuron and synaptic properties can be understood only in the context of
345 higher level network activity attributes. This complex interplay between low and high level features introduces emergent
346 phenomena that enrich the dynamical repertoire of the brain.

347 Materials and Methods

348 Neurons

349 *Neuron model*

350 Here we used the phenomenological model introduced by Izhikevich.³⁰ The sub-threshold dynamics of this neuron model
351 is defined by

352

$$\frac{dv}{dt} = 0.04v^2 + 5v + 140 - u + I$$

$$\frac{du}{dt} = a(bv - u)$$

353 and the spiking is described by if $v \geq 30\text{ mV}$, then $v \leftarrow c$ and $u \leftarrow u + d$

354 The variable v denotes the membrane potential and u denotes the activation of K^+ ionic current and inactivation of
355 Na^{2+} ionic current. The parameter a determines the time scale of the recovery variable and b defines the sensitivity of
356 u to the subthreshold fluctuations of v . c and d determine the reset values of v and u after spiking respectively. The
357 parameters used for the three types of neurons are given in **Table 1**.

358 *State-dependent Stochastic Bursting Neuron (SSBN)*

359 For the Izhikevich neuron model as well as other similar models, the various possible firing patterns are tightly coupled to
360 the $f - I$ curve of the neurons. Thus, the effects of firing patterns on network activity cannot be studied independently of
361 the neuronal firing rate. To overcome this problem, we introduce a novel neuron model, the State-dependent Stochastic
362 Bursting Neuron (SSBN). The SSBN neuron has identical membrane potential dynamics as the Leaky Integrate and Fire
363 (LIF) neuron given by

$$\tau_m \dot{v}_m = -v_m + I_{syn}$$

364 but the action-potential generation mechanism is stochastic. That is, whenever a predefined threshold u_{th} is reached,
365 b number of spikes are generated with probability $1/b$. The inter-spike-interval within the burst is constant (2 ms). The
366 membrane potential is reset only after all spikes of the burst are produced. Thus, the SSBN neuron produces bursts of
367 different lengths without altering the $f - I$ curve. The simulation parameters are defined in **Table 2**.

368 To make the above neuron model more biologically realistic, we let the number of spikes/burst b be a function of the
369 mean input current that a neuron receives. The mean input current, I_{inp} is a function of excitatory population firing rate, r

370 i.e., $\frac{r-r_{min}}{r_{max}} * B_{max}$, where r_{min} is the firing rate of the population with minimum number of spikes per burst and r_{max} is the
 371 population firing rate for the maximum number of spikes per burst in the inhibitory neurons, B_{max} . More specifically, b is
 372 drawn from a binomial distribution (every 1000 ms) $b \sim B(n, p)$ with mean $E[b] = f(I_{inp}) = np$, n denotes the maximum
 373 number of spikes per burst which is fixed to $n = 4$ and p is the probability of producing one spike. Thus the mean input
 374 current to the neuron I_{inp} affects the probability p . This we call the modified SSBN and this model is used in (Fig. 6
 375 (inset)) only.

376 Asynchronous state

377 In the stable asynchronous state the population activity is constant $r(t) = r_E = r_I = r_0$. The mean recurrent input that
 378 each neuron receives is therefore also constant and given by

$$I_{rec}(t) = J_E \cdot r_0 \cdot e \cdot \tau_s - J_I \cdot r_0 \cdot e \cdot \tau_s$$

We study the stability of the asynchronous state following a linear perturbation approach^{36,38}. A small oscillatory modulation of the stationary firing rate $r(t) = r_0 + r_1 e^{\lambda t}$ with $r_1 \ll 1$ and $\lambda = x + j\omega$ where ω is the modulation frequency leads to corresponding oscillation of the synaptic current

$$I_1 = \frac{J_E \cdot r_1 \cdot e \cdot \tau_s}{(1 + \lambda \cdot \tau_s)^2} e^{-\lambda d} - \frac{J_I \cdot r_1 \cdot e \cdot \tau_s}{(1 + \lambda \cdot \tau_s)^2} e^{-\lambda d} \quad (2)$$

The firing rate in response to an oscillatory input is given by

$$r_1 = \frac{I_1 \cdot r_0}{\sigma(1 + \lambda \tau_m)} \left(\frac{\frac{\partial U}{\partial y}(y_t, \lambda) - \frac{\partial U}{\partial y}(y_r, \lambda)}{U(y_t, \lambda) - U(y_r, \lambda)} \right) \quad (3)$$

379 The function U is given in terms of combinations of hypergeometric functions

$$\begin{aligned} U(y, \lambda) &= \frac{e^{y^2}}{\Gamma(\frac{1+\lambda\cdot\tau_m}{2})} F\left(\frac{1-\lambda\cdot\tau_m}{2}, \frac{1}{2}, -y^2\right) \\ &+ \frac{e^{y^2}}{\Gamma(\frac{\lambda\cdot\tau_m}{2})} F\left(1 - \frac{\lambda\cdot\tau_m}{2}, \frac{3}{2}, -y^2\right) \end{aligned}$$

In a recurrent network the modulation of the firing rate and the modulation of the synaptic input must be consistent. Combining (2) and (3) we get

$$J_E \cdot [R_E(\lambda) \cdot S_E(\lambda) - R_I(\lambda) \cdot S_I(\lambda) \cdot g] = 1 \quad (4)$$

with

$$R_P(\lambda) = \frac{r_0}{\sigma_P(1 + \lambda \tau_m)} \frac{\frac{\partial U}{\partial y}(y_t, \lambda) - \frac{\partial U}{\partial y}(y_r, \lambda)}{U(y_t, \lambda) - U(y_r, \lambda)}$$

and

$$S_P(\lambda) = \frac{e \cdot \tau_s}{(1 + \lambda \cdot \tau_s)^2}$$

where S_P is the synaptic response function for alpha-shaped postsynaptic currents

$$a(t) = e \cdot t / \tau_s \cdot e^{-t/\tau_s}$$

380 $P = E, I$ denotes either the excitatory or inhibitory population.

If the inhibitory population is bursting the synaptic response function is given by

$$S_I(\lambda) = \frac{e \cdot \tau_s (1 + \sum_{n=2}^B e^{-\lambda \cdot (n-1) \cdot T_b})}{(1 + \lambda \cdot \tau_s)^2}$$

381 where T_b is the length of the inter spike interval within a burst and B is the number of spikes in a burst. To compensate
382 for the increased PSP due to bursting, the recurrent inhibitory firing rate is divided by B .

The critical coupling values at which modes have marginal stability with frequency ω_i can then simply be computed
by

$$J_{E_i} = \frac{1}{R_E(\omega_i) \cdot S_E(\omega_i) - R_I(\omega_i) \cdot S_I(\omega_i) \cdot g}$$

383 The smallest value $J_{cr} = \min\{J_{E_i}\}$ is the critical coupling value at which the first complex pair of eigenvalues crosses
384 the imaginary axis and the system becomes unstable. The critical coupling values for different B is given by the dotted
385 line in Fig. 5A.

386 Networks

387 We generate networks of 4000 excitatory and 1000 inhibitory neurons randomly connected with a fixed probability of 0.1.
388 In all simulations the excitatory neurons are of the regular-spiking type (*RS*), while the inhibitory neurons are divided into
389 fast-spiking (*FS*) and bursting type (*BS*). The fraction of (*BS*) neurons is systematically varied between 0 and 1. For
390 each network we compute the fraction of BS neurons, given by $F = N_{BS}/N_I$, with $N_I = N_{FS} + N_{BS}$, where N_{FS}, N_{BS}, N_I are
391 the number of *FS*, *BS* and total number of inhibitory neurons respectively. Each neuron in the network receives poisson
392 background input of rate η . The ratio of the synaptic strength of the excitatory and inhibitory connections is denoted
393 by g .

394 **Hysteresis**

395 To test the network response when network activity and spikes per burst were mutually dependent we changed the number
396 of spikes per burst as a function of network firing rate. That is, at low firing rate, the network was composed only of
397 non-bursting neurons. However, as the network output firing rate was increased by slowly increasing the external input
398 was increased neurons started to burst. To implement a state-dependence of the burst size, we quantized the firing rate
399 of the excitatory neurons into five non-overlapping ranges ($[5 \times (B - 1) - 5 \times B]$ spikes/sec., where $B \in \{1,2,3,4,5\}$). The
400 SSB neuron generated B spikes depending on the level of the excitatory firing rate. To change the number of spikes per
401 burst, we estimated the input rate either in 3 sec (Fig. 6A) or 200 ms windows (Fig. 6B). To change the network firing
402 rate, we changed the external input to the network in steps of 100 spikes/sec every 3 sec (Fig. 6A) or 200 ms (Fig. 6B).
403 The external input was varied until the BS neurons reached a maximal burst size $B = 5$, after that the external input
404 was reduced with the same rate.

405 **Data Analysis**

We use the mean firing rate (v) and Fano factor (FF) to characterise the dynamical states of the networks. Mean firing rate is measured as the number of spikes per neuron per second. FF is used to quantify the synchrony in the network. The FF of a population is defined as

$$FF = \frac{\sigma^2[Z_i]}{\mu[Z_i]}$$

406 To obtain a reliable estimate of the population activity, the cumulative activity of the spike trains of all the neurons in
407 the network were binned in discrete time bins(bin width = 2 ms). Z_i is the population activity in a bin i . An increase in
408 positive correlation increased the $Variance[Z_i]$ and consequently the $FF[Z_i]$.

Coefficient of variation, CV , of the inter-spike interval distribution T of a neuron, is given by

$$CV = \frac{\sigma[T]}{\mu[T]}$$

409 The mean CV of the neurons in a population gives the regularity of neuronal spiking in the population.

410 **Spectral Entropy**

To quantify the degree of oscillatory activity in a network we compute the spectral entropy H_S , which is a measure of dispersion of spectral energy of a signal.⁵⁴ It is given by

$$H_S = \frac{-\sum_k P_k \log P_k}{\log N}$$

411 where P_k is the spectral power at frequency k and N is the total number of frequency bins considered. The power

412 spectrum is computed using a Fast-Fourier-Transform of the population activity v and normalized such that $\sum_k P_k = 1$.
413 A flat power spectrum, e.g. in the white noise case, has maximum spectral entropy, i.e. $H_S = 1$. By contrast,
414 a spectrum with all power concentrated in one frequency, e.g. periodic sine signal, has zero spectral entropy $H_S = 0$.
415 Therefore, the more oscillatory the activity dynamics is, the smaller H_S will be. In our simulations, the value of spectral
416 entropy ranged from 0.2 to 0.9.

417 While Fano factor is a good descriptor of the synchronicity in the network activity, it does not quantify network
418 oscillations. Whenever, we wanted to quantify the strength of the network oscillations specifically, we have used spectral
419 entropy.

420 **Simulation and Data Analysis Tools**

421 All network simulations are written in Python (<http://www.python.org>) and implemented in NEST (<http://www.nest-initiative.org>).⁵⁵ A temporal resolution of 0.1 ms is used for the intergration of the differential equations. Results were
422 analyzed using SciPy and NumPy libraries. Visualizations were done using Matplotlib.⁵⁶

424 **References**

425 **Acknowledgements**

426 We thank Dr.Christopher Kim for comments on an earlier version of this manuscript. This work was supported by the
427 German Federal Ministry of Education and Research (01GQ0830 to BFNT Freiburg/Tuebingen), FACETS-ITN (PITN-
428 GA-2009-237955) and the BrainLinks-BrainTools Cluster of Excellence funded by the German Research Foundation
429 (DFG #EXC 1086). AK and AS acknowledge INTERREG IV Rhin superieur program and European Funds for Regional
430 Development (FEDER) through the project TIGER A31. We also acknowledge the use of the computing resources
431 provided by the Black Forest Grid Initiative and the bwGRiD (<http://www.bw-grid.de>), member of the German D-Grid
432 initiative, funded by the Ministry for Education and Research and the Ministry for Science, Research and Arts Baden-
433 Wuerttemberg.

434 **Additional Information**

435 The project was funded in part by following funding agencies: Bundesministerium fuer Forschung und Technologie
436 (German Ministry for Research and Technology) - 01GQ0830 [to Ad Aertsen and Arvind Kumar]; Deutsche Forschungs-
437 gemeinschaft (DFG) - EXC 1086 [to Ad Aertsen and Arvind Kumar]; Ajith Sahasranamam was partially funded by the
438 FACETS-ITN (PITN-GA-2009-237955). AK and AA also acknowledge the INTERREG IV Rhin Superieur Program and
439 the European Funds for Regional Development (FEDER) through the project TIGER A31. We also acknowledge the
440 use of the computing resources provided by the Black Forest Grid Initiative and the bwGRiD (<http://www.bw-grid.de>),
441 member of the German D-Grid initiative, funded by the Ministry for Education and Research and the Ministry for Science,
442 Research and Arts Baden-Wuerttemberg.

443 **Competing financial interest**

444 There is NO Competing Interest.

445 **Author Contributions**

446 Conceived and designed the experiments: AS, IV, AA, AK. Performed the experiments: AS, IV. Analyzed the data: AS,
447 IV. Contributed reagents/ materials/analysis tools: AK. Contributed to the writing of the manuscript: AS, IV, AA, AK.

448 **References**

- 449 1. Markram, H. *et al.* Interneurons of the neocortical inhibitory system. *Nat Rev Neurosci* **5**, 793–807 (2004).
- 450 2. Luo, L., Callaway, E. M. & Svoboda, K. Genetic dissection of neural circuits. *Neuron* **57**, 634–60 (2008).
- 451 3. Defelipe, J. *et al.* New insights into the classification and nomenclature of cortical gabaergic interneurons. *Nat Rev Neurosci* **14**, 202–216 (2013).
- 452 4. Wichterle, H., Gifford, D. & Mazzoni, E. Mapping neuronal diversity one cell at a time. *Science* **341**, 726–727 (2013).
- 453 5. Neske, G. T., Patrick, S. L. & Connors, B. W. Contributions of diverse excitatory and inhibitory neurons to recurrent network activity in cerebral cortex. *J Neurosci* **35**, 1089–1105 (2015).
- 454 6. Yizhar, O. *et al.* Neocortical excitation/inhibition balance in information processing and social dysfunction. *Nature* **477**, 171–8 (2011).
- 455 7. Sohal, V. S., Zhang, F., Yizhar, O. & Deisseroth, K. Parvalbumin neurons and gamma rhythms enhance cortical circuit performance. *Nature* **459**, 698–702 (2009).
- 456 8. Cardin, J. A. *et al.* Driving fast-spiking cells induces gamma rhythm and controls sensory responses. *Nature* **459**, 663–7 (2009).
- 457 9. Wilson, N. R., Runyan, C. A., Wang, F. L. & Sur, M. Division and subtraction by distinct cortical inhibitory networks in vivo. *Nature* **488**, 343–348 (2012).
- 458 10. Denker, M., Timme, M., Diesmann, M., Wolf, F. & Geisel, T. Breaking synchrony by heterogeneity in complex networks. *Phys Rev Lett* **92**, 074103–1–074103–4 (2004).
- 459 11. Padmanabhan, K. & Urban, N. N. Intrinsic biophysical diversity decorrelates neuronal firing while increasing information content. *Nat Neurosci* **13**, 1276–82 (2010).
- 460 12. Pinto, L. & Dan, Y. Cell-Type-Specific Activity in Prefrontal Cortex during Goal-Directed Behavior. *Neuron* **87**, 437–450 (2015).
- 461 13. Diester, I. *et al.* An optogenetic toolbox designed for primates. *Nat Neurosci* **14**, 387–97 (2011).
- 462 14. Achard, P. & Schutter, E. D. Complex parameter landscape for a complex neuron model. *PLoS Comput Biol* **2**, e94 (2006).
- 463 15. Prinz, A. A., Bucher, D. & Marder, E. Similar network activity from disparate circuit parameters. *Nat Neurosci* **7**, 1345–1352 (2004).
- 464 16. Marder, E. & Taylor, A. L. Multiple models to capture the variability in biological neurons and networks. *Nature* **477**, 133–138 (2011).

- 478 17. Ascoli, G. A. *et al.* Petilla terminology: nomenclature of features of GABAergic interneurons of the cerebral cortex.
479 *Nature Reviews Neuroscience* **9**, 557–568 (2008).
- 480 18. Gupta, A., Wang, Y. & Markram, H. Organizing principles for a diversity of GABAergic interneurons and synapses
481 in the neocortex. *Science* **287**, 273–278 (2000).
- 482 19. Jarsky, T., Mady, R., Kennedy, B. & Spruston, N. Distribution of bursting neurons in the CA1 region and the
483 subiculum of the rat hippocampus. *J Comp Neurol* **506**, 535–547 (2008).
- 484 20. Larkum, M. E., Zhu, J. J. & Sakmann, B. Dendritic mechanisms underlying the coupling of the dendritic with the
485 axonal action potential initiation zone of adult rat layer 5 pyramidal neurons. *J Physiol* **533**, 477–466 (2001).
- 486 21. Womelsdorf, T., Ardid, S., Everling, S. & Valiante, T. A. Burst firing synchronizes prefrontal and anterior cingulate
487 cortex during attentional control. *Current Biology* 1–9 (2014).
- 488 22. Sanabria, E. R., Su, H. & Yaari, Y. Initiation of network bursts by Ca²⁺-dependent intrinsic bursting in the rat
489 pilocarpine model of temporal lobe epilepsy. *J Physiol (London)* **532**, 205–216 (2001).
- 490 23. Tachibana, Y., Iwamuro, H., Kita, H., Takada, M. & Nambu, A. Subthalamo-pallidal interactions underlying
491 parkinsonian neuronal oscillations in the primate basal ganglia. *Eur J Neurosci* **34**, 1470–1484 (2011).
- 492 24. Markram, H., Wang, Y. & Tsodyks, M. Differential signaling via the same axon of neocortical pyramidal neurons.
493 *Proc Natl Acad Sci USA* **95**, 5323–5328 (1998).
- 494 25. Wittenberg, G. M. & Wang, S. S.-H. Malleability of spike-timing-dependent plasticity at the ca3-ca1 synapse. *J*
495 *Neurosci* **26**, 6610–6617 (2006).
- 496 26. Kumar, A. & Mehta, M. R. Frequency dependent changes in NMDA-dependent synaptic plasticity. *Front Comput.*
497 *Neurosci* **5** (2011).
- 498 27. Wang, X.-J. Neurophysiological and computational principles of cortical rhythms in cognition. *Physiological Reviews*
499 **90**, 1195–268 (2010).
- 500 28. Bogaard, A., Parent, J., Zochowski, M. & Booth, V. Interaction of cellular and network mechanisms in spatiotemporal
501 pattern formation in neuronal networks. *J Neurosci* **29**, 1677–1687 (2009).
- 502 29. Krahe, R. & Gabbiani, F. Burst firing in sensory systems. *Nat. Rev. Neurosci.* **5**, 13–23 (2004).
- 503 30. Izhikevich, E. M. Simple mode of spiking neurons. *IEEE Trans. on Neural Networks* **14**, 1569–1572 (2003).
- 504 31. Uhlhass, P. J. *et al.* Neural synchrony in cortical networks: history, concept and current status. *Front Integr Neurosci*
505 **3**, 1–19 (2009).
- 506 32. Fries, P. A mechanism for cognitive dynamics: neuronal communication through neuronal coherence. *Trends in*
507 *Cognitive Sciences* **9**, 474–480 (2005).
- 508 33. Buzsáki, G. & Wang, X.-J. Mechanisms of gamma oscillations. *Annu Rev Neurosci* **35**, 203–225 (2012).

- 509 34. Brunel, N. & Wang, X.-J. What determines the frequency of fast network oscillations with irregular neural discharges?
510 i. synaptic dynamics and excitation-inhibition balance. *J Neurophysiol* **90**, 415–430 (2003).
- 511 35. Ledoux, E. & Brunel, N. Dynamics of networks of excitatory and inhibitory neurons in response to time-dependent
512 inputs. *Front Comput Neurosci* **5**, 1–17 (2011).
- 513 36. Brunel, N. & Hakim, V. Sparsely synchronized neuronal oscillations. *Chaos* **18**, 015113 (2008).
- 514 37. Tiesinga, P. & Sejnowski, T. J. Cortical enlightenment: Are attentional gamma oscillations driven by ping or pong?
515 *Neuron* **63**, 727–732 (2009).
- 516 38. Brunel, N. & Hansel, D. How noise affects the synchronization properties of recurrent networks of inhibitory neurons.
517 *Neural Computation* **18**, 1066–110 (2006).
- 518 39. Brunel, N. Dynamics of sparsely connected networks of excitatory and inhibitory spiking neurons. *J Comput Neurosci*
519 **8**, 183–208 (2000).
- 520 40. Kumar, A., Schrader, S., Aertsen, A. & Rotter, S. The high-conductance state of cortical networks. *Neural
521 Computation* **20**, 1–43 (2008).
- 522 41. Hahn, G., Bujan, A. F., Frégnac, Y., Aertsen, A. & Kumar, A. Communication through resonance in spiking neuronal
523 networks. *PLoS Comput Biol* 1–16 (2014).
- 524 42. vanVreeswijk, C. & Sompolinsky, H. Chaos in neuronal networks with balanced excitatory and inhibitory activity.
525 *Science* **274**, 1724–1726 (1996).
- 526 43. Stern, M., Sompolinsky, H. & Abbott, L. F. Dynamics of random neural networks with bistable units. *Phys. Rev. E*
527 **90**, 1–7 (2014).
- 528 44. Amit, D. & Brunel, N. Model of global spontaneous activity and local structured activity during delay periods in the
529 cerebral cortex. *Cereb. cortex* **7**, 237–252 (1997).
- 530 45. Mongillo, G., Hansel, D. & van Vreeswijk, C. Bistability and spatiotemporal irregularity in neuronal networks with
531 nonlinear synaptic transmission. *Phys. Rev. Lett.* **108**, 158101 (2012).
- 532 46. Schnepel, P., Kumar, A., Zohar, M., Aertsen, A. & Boucsein, C. Physiology and impact of horizontal connections
533 in rat neocortex. *Cerebral Cortex* 1–18 (2014).
- 534 47. Bonifazi, P. et al. Gabaergic hub neurons orchestrate synchrony in developing hippocampal networks. *Science* **326**,
535 1419–1424 (2009).
- 536 48. Vlachos, I., Aertsen, A. & Kumar, A. Beyond statistical significance: Implications of network structure on neuronal
537 activity. *PLoS Comput Biol* **8**, e1002311 (2012).
- 538 49. Kumar, A., Vlachos, I., Aertsen, A. & Boucsein, C. Challenges of understanding brain function by selective modulation
539 of neuronal subpopulations. *Trends in Neurosciences* **36**, 579–586 (2013).

- 540 50. Gutierrez, G. J. & Marder, E. Rectifying electrical synapses can affect the influence of synaptic modulation on output
541 pattern robustness. *J Neurosci* **33**, 13238–13248 (2013).
- 542 51. Connors, B. W. & Gutnick, M. J. Intrinsic firing patterns of diverse neocortical neurons. *Trends in Neurosciences*
543 **13**, 99–104 (1990).
- 544 52. Karimi, F. & Holme, P. Threshold model of cascades in empirical temporal networks. *Physica A: Statistical Mechanics
545 and its Applications* **392**, 3476–3483 (2013).
- 546 53. Vogels, T. P., Sprekeler, H., Zenke, F., Clopath, C. & Gerstner, W. Inhibitory plasticity balances excitation and
547 inhibition in sensory pathways and memory networks. *Science* **334**, 1569–1573 (2011).
- 548 54. Blanco, S., Garay, A. & Coulombe, D. Comparison of frequency bands using spectral entropy for epileptic seizure
549 prediction. *ISRN Neurol* **2013**, 287327 (2013).
- 550 55. Gewaltig, M.-O. & Diesmann, M. Nest (neural simulation tool). *Scholarpedia* **2**, 1430 (2007).
- 551 56. Hunter, J. D. Matplotlib: A 2d graphics environment. *Computing In Science & Engineering* **9**, 90–95 (2007).
- 552 57. Gourévitch, B. & Eggermont, J. J. A nonparametric approach for detection of bursts in spike trains. *J Neurosci
553 Methods* **160**, 349–58 (2007).

Neuron type	a	b	c	d
Regular spiking(RS)	0.2	0.2	-65	2
Fast spiking(FS)	0.1	0.2	-65	2
Bursting(BS)	0.02	0.2	-50	2

Table 1. Izhikevich neuron parameters

Name	Value	Description
C_m	250pF	Membrane capacitance
τ_m	10ms	Membrane Time Constant
V_{th}	-55mV	Firing threshold
V_{reset}	-70mV	Reset potential
τ_{ref}	2ms	Refractory period
τ_{syn}	2ms	Rise time of alpha function
d	1.5ms	synaptic delay
J_E	$0.05 - 0.1\text{mV}$	Excitatory weight
J_I	$0.1 - 0.9\text{mV}$	Inhibitory weight

Table 2. Simulation parameters

554 **Supplementary figures**

Figure 1. Effect of increasing the fraction of bursting neurons in the inhibitory population on the stability of γ band oscillations. (A) Schematic of the network. (B) Spiking activity in a network with only FS neurons constituting the inhibitory population. A clear oscillatory activity is seen in the excitatory neurons (blue dots) and inhibitory FS neurons (orange dots) ($g = 7.1, \eta = 2.8 \times 10^4 \text{ sp/s}, J_E = 0.1 \text{ mV}$) . (C) Spiking activity in a network with only BS neurons (gray dots) constituting the inhibitory population. All other network parameters are the same as for the activity shown in B. Inhibitory BS neurons weaken network oscillations. (D) Stability of the oscillations (quantified by the Spectral Entropy) of excitatory neurons as a function of the fraction of BS neurons. ($g = 7.1$) (E) Spectral entropy, excitatory and inhibitory (FS+BS) population firing rate as a function of the external input (η) to a network with 40% BS and 60% FS inhibitory neurons. (F) Oscillation frequencies as a function of the external input. For a fixed fraction of BS neurons, spectral entropy remained unchanged while the oscillation frequency and the firing rate of the neurons increased.

Figure 2. Effect of increasing the fraction of bursting neurons(F) in the inhibitory population on synchrony in the network activity. (A) Synchrony (measured as Fano Factor) in the excitatory neurons as a function of the ratio of recurrent inhibition and excitation (g) and external excitatory input (η), for 0% bursting neurons in the inhibitory population. (B) Same as in A when 50% inhibitory neurons are bursting type. (C) Same as in A when all inhibitory neurons are bursting type. (D) Summary of the changes induced by increasing fraction of bursting neurons on the different activity states of the network. (E) Four representative changes in the network synchrony as the fraction of bursting neurons is increased from 0 to 100% corresponding to the crosses in D. ($J_E = 0.1\text{mV}$, $d = 1.5\text{ms}$)

Figure 3. The state-dependent stochastic bursting neuron. (A) Izhikevich neuron producing regular spiking (RS), fast spiking (FS) and Bursting (BS) firing patterns for different values of the neuron parameters a, b, c and d . (B) The firing rate response of the neuron types for different poisson input rates. (C) Firing patterns of the State-dependent Stochastic Bursting Neuron (SSBN) model with varying number of spikes per burst for the same value of constant external DC input (top to bottom). (D) The firing rate response curve of the SSBN for different number of spikes per burst, for external Poisson input of different rates.

Figure 4. Mechanism-I by which spike bursting destroys network oscillations. **(A)** The network which is initially in an oscillatory state switches to a non-oscillatory state with the replacement of FS neurons (orange dots) with the BS neurons (grey dots) in the inhibitory population. The blue dots show the excitatory spikes and the dark blue line is the z-scored PSTH of the excitatory activity. The light brown stripes correspond to the crest of the oscillatory cycles of the excitatory population when the network consisted of only FS inhibitory neurons. The number of additional spikes that fall within the stripes is calculated (num_{add}) added ($g = 12, d = 2\text{ms}, \eta = 11500\text{sp/s}, F = 0.4$). **(B)** A schematic to depict how the addition of additional inhibitory spikes (red dots) when the inhibitory oscillatory cycle wanes makes the oscillatory activity unstable in an ING oscillation. The excitatory population (blue dots) oscillates in the window of opportunity provided by the inhibitory population (orange dots). The red dots indicate the additional inhibitory spikes that are added. **(C)** Same as in **(B)**, except that the oscillations are PING driven. **(D)** PSTHs of the excitatory population shows the changes after the addition of the num_{add} additional spikes in the inhibitory population. When the additional spikes are added when the inhibitory oscillatory cycle tapers off there is maximum disturbance of succeeding oscillatory cycles (blue line). When the same number of spikes are added at the peak of the preceding oscillatory cycle, there is minimal effect on the subsequent oscillatory cycle (dark blue line). The pale blue line shows the baseline activity when no spikes are added ($g = 12, d = 2\text{ms}, \eta = 11500\text{sp/s}$). **(E)** PSTHs of the excitatory population affected by additional spikes in a PING driven oscillation ($g = 7, d = 1.5\text{ms}, \eta = 20000\text{ sp/s}$).

Figure 5. Mechanism-II by which spike bursting enhances oscillations. **(A)** In the phase space of excitatory synaptic strength (J_E) and the number of spikes per burst(F), the bifurcation line (dotted black line) between the oscillatory and non-oscillatory states is the J_{cr} value calculated analytically (for input $mean = 14mV$ and $\sigma = 6mV$. $d = 5ms$, $t_{syn} = 1ms$ and $V_{th} = 20mV$). When the FS neurons in the inhibitory population are replaced by BS neurons the number of spikes per burst of the neurons in the inhibitory population is altered and the J_{cr} value drops. A network in an initially asynchronous state can continue to remain asynchronous with the addition of BS neurons if the J_E values are less than J_{cr} for $F = 4$ (bottom panels). The network can transition from asynchronous to synchronous states with the change in F , if the J_E is more than J_{cr} for $F = 4$ (middle panels). Also, a network in an oscillatory state for $F = 1$ remains oscillatory for $F = 4$ (top panels). **(B)** Instead of replacing the entire FS population with BS neurons, different proportions of the inhibitory population were changed for the networks in panel **A** with $F = 1$. It is observed that the addition of 25% BS neurons in a network in a synchronous state, destroys oscillations due to Mechanism -I. **(C)** The change in the firing rate of the excitatory population for transitions in **A** while number of spikes per burst are changed.

Figure 6. Bursting introduces multi-stability and hysteresis in the network dynamics. **(A)** The increase in firing rate due to increase in external input and change in the burstiness of the neuron (dashed grey lines) is shown. The simulation protocol to generate this neuronal network hysteresis is described in Methods. It is seen that the onward (blue line) and return (brown line) curves do not trace the same path indicating the state dependence of the effect of the single neuron firing pattern on the network. The grey dots show a similar hysteresis loop for a network in which the burstiness of only 20% of the inhibitory neurons is changed. The inset plot shows the simultaneous change of the firing rate of the network and the burstiness of the modified-SSBN after given an initial perturbation of additional external input of 200 spikes/sec. The burstiness of the inhibitory neurons (as defined by the state variable (see Methods)) increases with the excitatory population firing rate. The increase in bursting in turn increases the population firing rate. This self-propelling mechanism continues till the single neurons produce the maximum number of spikes per burst ($B = 5$). **(B)** This panel is similar to **A**, but the firing rate estimate of the excitatory population is made over a time window of 200ms. The number of spikes per burst increase by 2 for every crossing of the firing rate threshold.

Figure 7. (A) The flowchart shows the different aspects that we glean from the results to establish the relationship between the single neuron properties and network dynamics (black lines). The description of the network effects of bursting through the two mechanisms was achieved by separating the effect of $f - I$ curves from that of the firing patterns by using SSB neurons. The single neuron firing pattern made dependent on the network dynamics resulted in hysteresis. The gray lines show the unexplored facets of the relationship between the two in the manuscript. (B) This schematic summarizes how the two mechanisms control the oscillatory activity in the network. The addition of BS neurons in an oscillating system gives rise to a recurrent noise and destroys the fine temporal balance between E and I populations that give rise to oscillations and quench them. Mechanism-II shifts the bifurcation line in the phase space by reducing the J_{cr} with the addition of BS neurons.

Figure S1. Increased bursting reduces the frequency of input oscillations that can be tracked. In unconnected networks of different number of modified-SSBNs, we test how well sinusoidally modulated input of different frequencies could be followed by the population. For higher input frequencies, it is seen that for increased number of spikes per burst are less able to follow the input. The rasters and the z-scored PSTHs for different number of spikes per burst for a fixed sinusoidal input (120 Hz) are shown in (A) and (B). (C) For a fixed size of the neuron ensemble ($N = 100$) it is observed that the normalized power of the peak frequency drops and saturates at a very low value (≈ 0) for higher frequencies of the sinusoidally modulated input. (D) The map shows the maximum frequency of the input that can be tracked by different combinations of number of independent neurons in the population and the number of spikes per burst. While the value of the frequency drops with the increase in the number of spikes per burst, it can be compensated for by increasing the number of neurons in the ensemble.

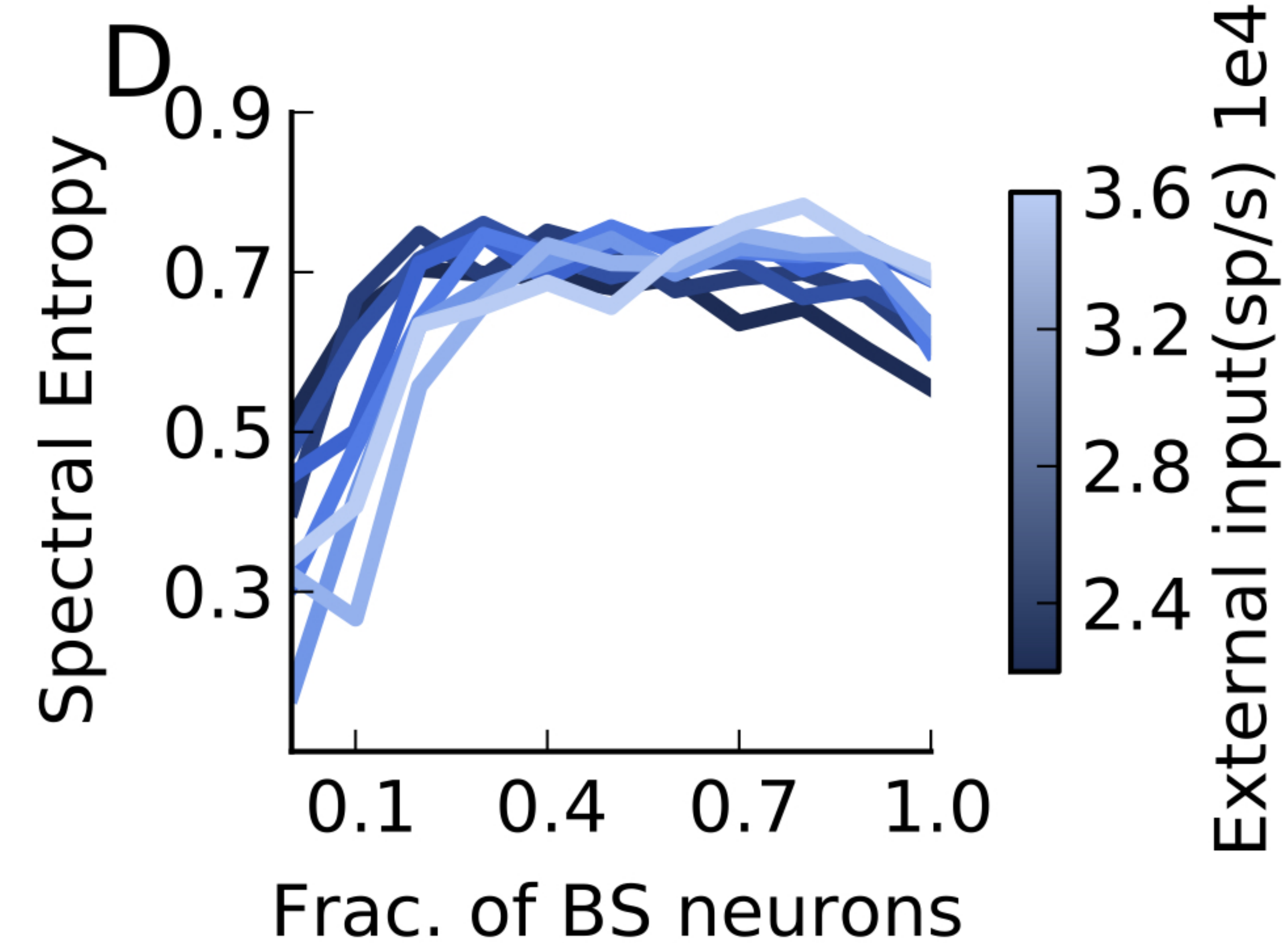
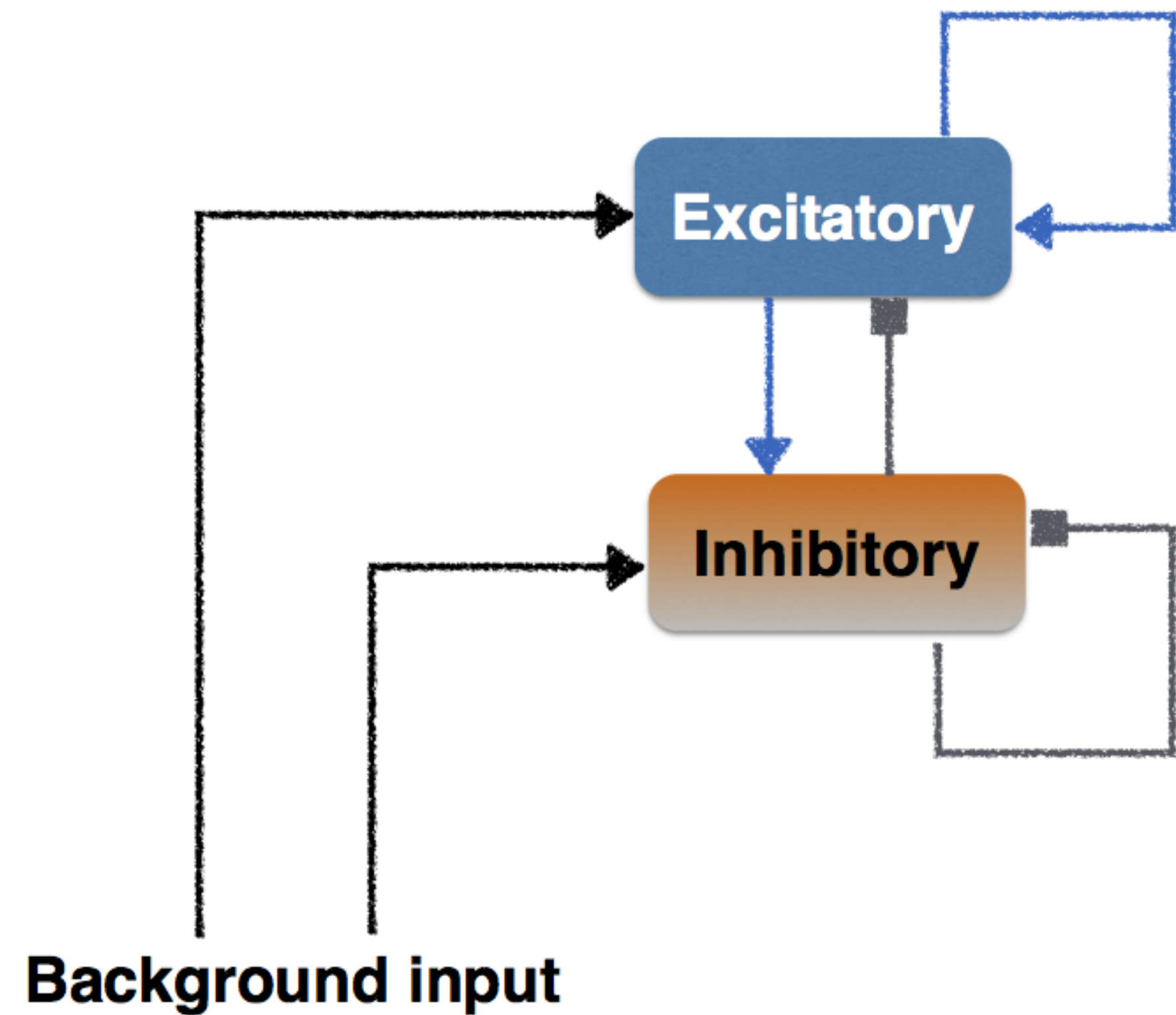
Figure S2. Figure caption continued on the following page

Figure S2. Effect of addition of bursting neurons on the state of network composed of SSBN. (A) Evolution of spectral entropy(H_S) for a network which is initially synchronous and changes to being asynchronous with the addition of bursting neurons, added ($g = 11, d = 2\text{ms}, \eta = 10500 - 11500 \text{ sp/s}, J_E = 0.1 \text{ mV}$). (B) a network in an asynchronous state that continues to remain asynchronous with the addition of bursting neurons ($g = 5, d = 2.0\text{ms}, \eta = 4000 - 5000 \text{ sp/s}, J_E = 0.04 \text{ mV}$) , C qualitatively synchronous activity can remain synchronous even when inhibitory neuron firing patterns are changed ($g = 8, d = 4\text{ms}, \eta = 8500 - 9500 \text{ sp/s}, J_E = 0.1 \text{ mV}$) and (D) an initially asynchronous activity in the network that becomes synchronous with the addition of bursting neurons ($g = 6, d = 2\text{ms}, \eta = 4500 - 5500 \text{ sp/s}, J_E = 0.1 \text{ mV}$). (E) The Fano Factor values of the different transitions are plotted against the changes in the fraction of bursting neurons. The different colours correspond to the different state transitions observed (colours marked in the titles of A,B,C and D.).(F) The rasters illustrating the four types of transitions are shown in a phase space of FF and the difference in H_S . The difference in H_S is the difference in spectral entropy between the initial and final points of each transitions. The initial rasters are marked in yellow and the final rasters are marked in black in the corresponding panels A,B,C and D. The FF values marked are the FF values of the initial points.

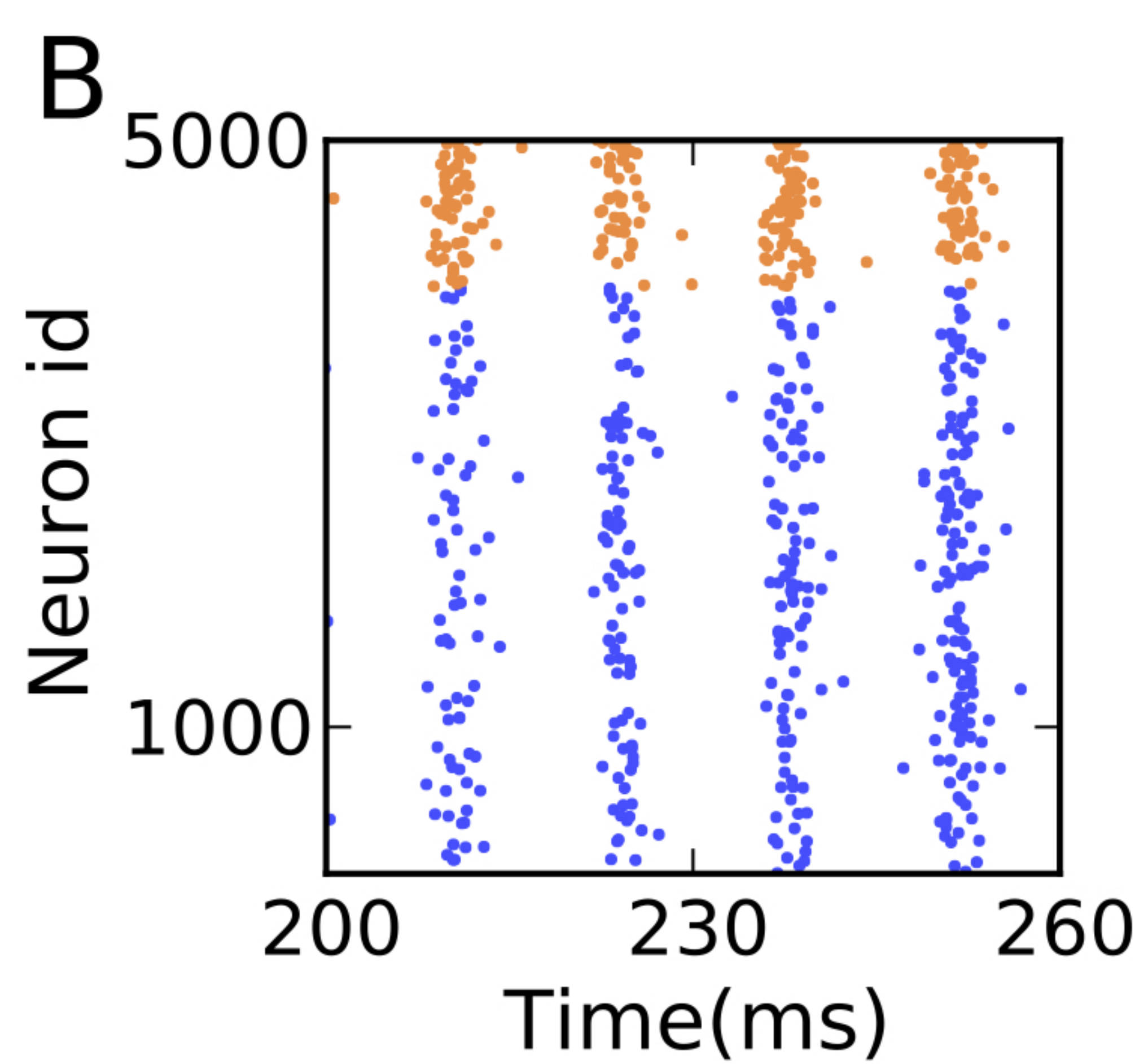
Figure S3. A simple network producing an external input induced spiking of a presynaptic BS population. This BS population acted as the inhibitory presynaptic input to a regular LIF neuron. The membrane potential of this LIF neuron was maintained very close to the threshold by an external poissonian input. The percentage change in the variance of the membrane potential (**A**) and firing rate (**B**) of the postsynaptic LIF neuron with the varying number of spikes per burst in the presynaptic SSBN population is plotted. The increase in the size of the presynaptic population decreased the amount of changes in the variance of the membrane potential and the firing rate of the post-synaptic LIF with the change in the number of spikes per burst.

Figure S4. Burstiness of single neurons changes with network state. The number of spikes per burst that a BS neuron(Izhikevich model) produces depends on the state of the network. To quantify the burstiness of a neuron we use the Bursting Index.⁵⁷ This measure assigns a rank R_n to every interspike interval (ISI) of a spike train. The lowest value of an ISI has zero rank. If the ISIs are independent, the value of each ISI can be considered to be a random number drawn from a uniform distribution between 1 and N, where N is the total number of ISIs. If a spike train contains a burst, then this assumption does not hold anymore. The Bursting Index is equivalent to the Rank Surprise (RS) statistic, which captures the discrepancy between the case of having independent and uniformly distributed sequence of variables R_n, \dots, R_{n+q-1} and the actual outcome in the case of a burst consisting of q number of spikes. It is given given by $RS = -\log(P(T_q \leq r_n + \dots + r_{n+q-1}))$ where r_n is the observed value of rank R_n . T_q is the sum of q discrete uniform variates between 1 and N. In the above figure, the average bursting index of BS neurons for different η and g values are shown in a randomly connected network of excitatory-BS neurons (Izhikevich model)

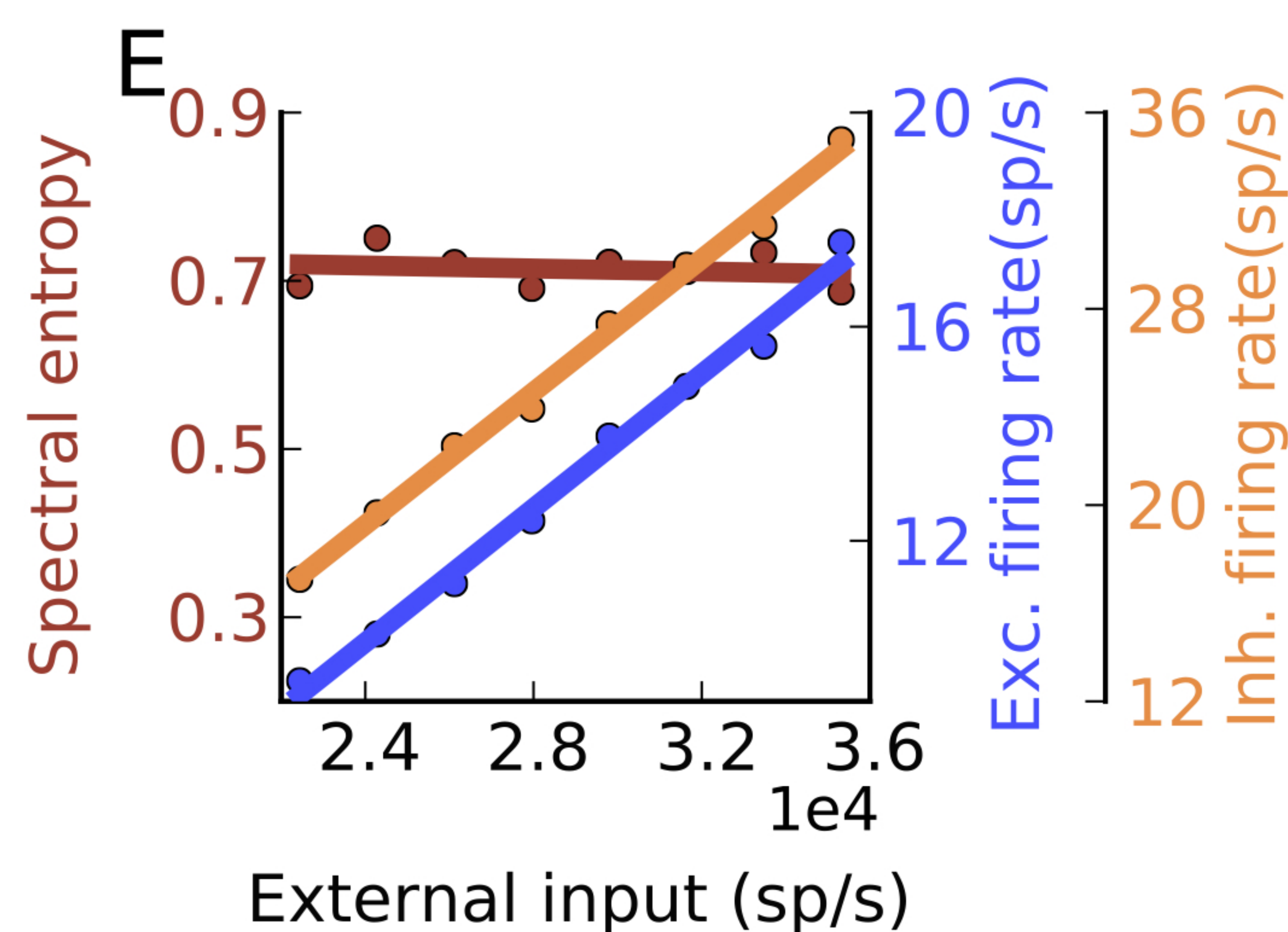
A



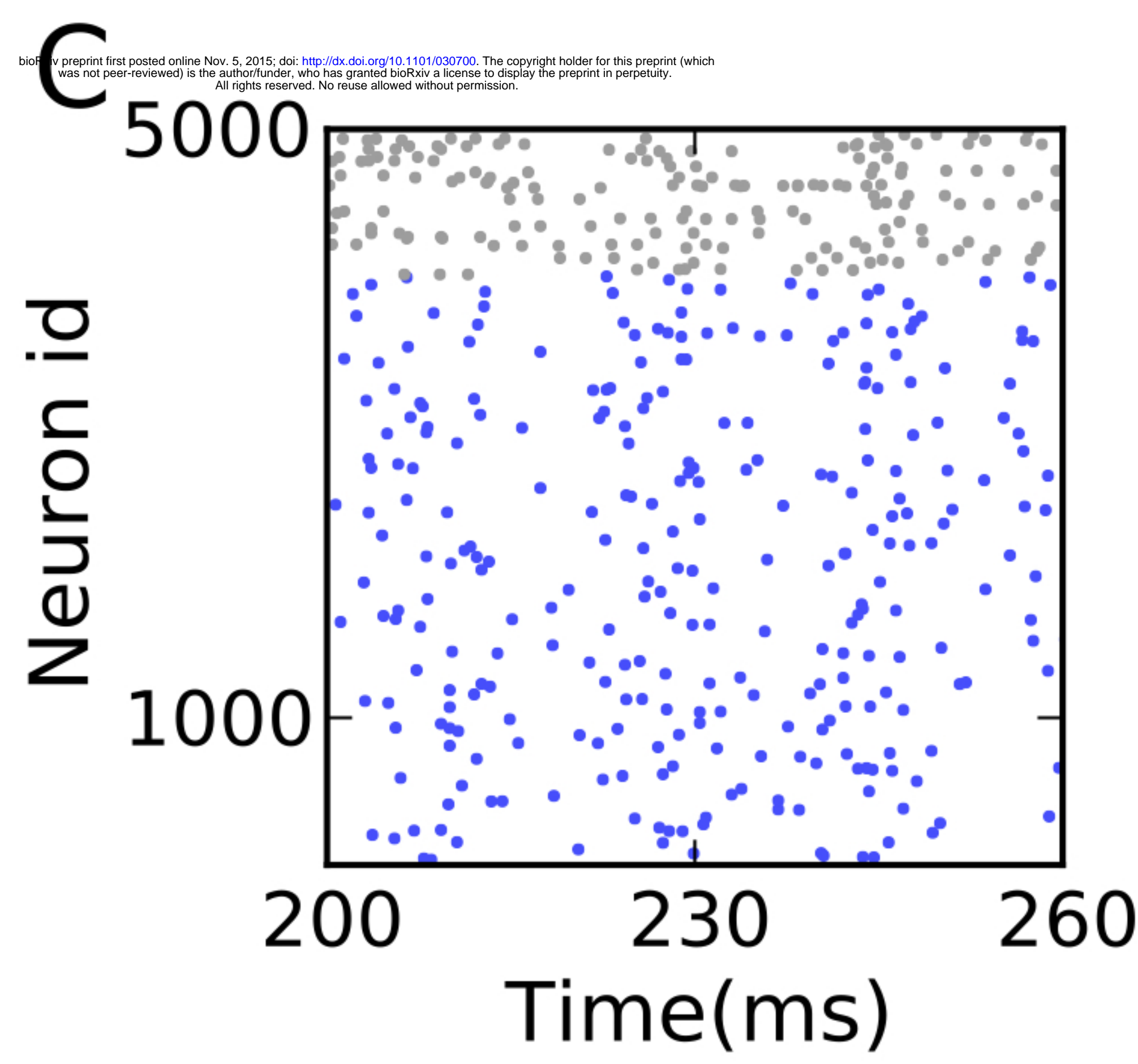
B



E



C



F

